Declining Water Resources in the Anduña River Basin of Western Pyrenees: Land Abandonment or Climate Variability?

Nerea Bilbao-Barrenetxea[a,d,*], Patricia Jimeno-Sáez[b], Francisco José Segura-Méndez[b], Gerardo Castellanos-Osorio[b], Adrián López-Ballesteros[b], Sergio Henrique Faria[a,c], Javier Senent-Aparicio[b]

[a] *Basque Centre for Climate Change (BC3), Leioa, 48940 , Spain,*
[b] *Department of Civil Engineering, Catholic University of San Antonio, Campus de Los Jerónimos s/n, Murcia, 30107, Spain,*
[c] *IKERBASQUE, Basque Foundation for Science, Plaza Euskadi 5, Bilbao, 48009, Spain,*
[d] *Faculty of Science and Technology. University of the Basque Country UPV/EHU, Leioa, 48940 , Spain,*

Abstract

Study Region:

Mountains play a crucial role in supplying water for consumption, irrigation, and hydroelectric power. However, they are highly vulnerable to climate change. The Pyrenees exemplify a mountainous region undergoing significant changes, notably in land-use practices, with a significant shift towards forest cover.

Study Focus:

We use the SWAT model, to analyse in depth two factors that most influence the hydrological cycle: land-use change and climate variability. The model is calibrated and validated using daily streamflow for the periods 1992–2004 and 2005– 2018. The following results were obtained for both periods: an NSE of 0.51, an R2 of 0.72, and a PBIAS of –12.67 % for the calibration period and an NSE of 0.55, an R2 of 0.75, and a PBIAS of –16.49 % for the validation period, indicating that the model accurately represented the daily streamflow. Subsequently, we designed three scenarios based on com-

*Corresponding author
Email address: nerea.bilbao@bc3research.org (Nerea Bilbao-Barrenetxea)

binations of historical data to quantify the contribution of each factor.

New Hydrological Insights for the Region:

Comparing the scenarios confirms the downward trend of streamflow in the region and provides quantitative information on the influence of each factor on this decline. Notably, that land-use changes account for 41.4 % almost as much as the climate variability. Furthermore, we observed an increase in the frequency and magnitude of floods with an increase in flood parameters of about 40%. The alteration of these parameters is slightly mitigated by reforestation, leading to a decrease of 5%.

Keywords: land abandonment; reforestation; climate variability; SWAT; Pyrenees; water resources

1. Introduction

Mountains play a key role in freshwater storage, providing half of the world's population with water resources (Viviroli et al., 2007; Immerzeel et al., 2020). However, in recent decades, major changes have been observed in the variables and processes that shape the hydrological cycle, such as climate variables, land cover, snow cover, and soil properties, which irremediably impact the availability of water resources downstream (Arnell, 1999; Beguería et al., 2003; Stewart et al., 2005). The vulnerability of mountain regions is most evident in the case of the Pyrenees, located between the Mediterranean and Atlantic climates, which are experiencing significant increases in temperature and changes in precipitation regimes (Amblar-Francés et al., 2020). Similarly, snow cover and its melting and accumulation, closely interconnected with streamflow in the Pyrenees region (López-Moreno and García-Ruiz, 2004), are also altered in the context of climate change. Climate variability over the years has resulted in changes in the timing and magnitude of the streamflow.

Land–use changes are a pivotal factor influencing hydrological processes. Since the 1950s mountain regions such as the Pyrenees (Poyatos et al., 2003) and the Alps (Ranzi et al., 2002; Tasser et al., 2007) have experienced significant changes in land–use consisting of arable land abandonment and subsequent reforestation, especially in the mid-altitude regions, (i.e. those below 1600 m (García-Ruiz et al., 1995)).This progressive greening process has spread worldwide in the last three decades (Zeng et al., 2016; FAO, 2014). Afforestation and agricultural land abandonment notably impact evapotranspiration (Haria and Price, 2000; Rasouli et al., 2019a), interception, and other hydrological processes (Beguería et al., 2003). Numerous studies have explored the implications of these changes for the hydrological cycle, revealing significant reductions in streamflow as a consequence of revegetation (Rasouli et al., 2019b; Guo et al., 2024; Ranzi et al., 2017), with potential repercussions on mountain ecosystem services (Boix-Fayos et al., 2020). Furthermore, alterations in land–use influence flood and drought regimes (Ranzi et al., 2002). Several studies indicate potential flood mitigation effect resulting from revegetation-based management practices (Nadal-Romero et al., 2021; Valente et al., 2021).

The influence of these factors on hydrological cycle alterations in the Pyrenees has been extensively studied. López-Moreno et al. (2008) observed a negative discharge trend in certain Pyrenean basins, accompanied by increased potential evapotranspiration (PET), suggesting a reduction in runoff generation capacity due to climate factors. However, climate drivers alone do not fully account for the observed decrease in water discharges (López-Moreno et al., 2011). Additionally, reductions in snow cover resulting from global warming have notably impacted hydrological regimes (López-Moreno and García-Ruiz, 2004; Sanmiguel-Vallelado et al., 2017). However, numerous researchers primarily attribute the negative water yield trend in Pyrenean watersheds to land-use changes (Juez et al., 2022; Lorenzo-Lacruz et al., 2012; Martínez-Fernández et al., 2013).

Hence, this study endeavours to isolate and quantify the influence of climate variability and land-use changes on the hydrological cycle. This analytical approach has been frequently employed, leveraging the SWAT model, a physically-based distributed hydrological model (Senent-Aparicio et al., 2018; Zhang et al., 2017; Yin et al., 2017). This methodology has been applied to several basins within the Iberian Peninsula (Molina-Navarro et al., 2014; Senent-Aparicio et al., 2018). For example, Senent-Aparicio et al. (2018) evaluated the impacts of climate variability and reforestation efforts on water resources in the headwaters of the Segura River Basin. Similarly, Molina-Navarro et al. (2014) investigated the effects of climate change and land-use management scenarios on water discharge and quality in the Pareja Reservoir, situated within the upper Tagus River Basin.

The indicators included in the Indicators of Hydrological Alteration in Rivers (IAHRIS, (Martinez and Fernández, 2010)) software have been used to analyse the impact of land abandonment on water resources. This software assesses 22 indices concerning the magnitude, variability, seasonality and duration of the three main elements of the flow regime: usual values, floods and droughts (Mellado-Díaz et al., 2019). The tool was developed in Spain to address the requirements of the European Water Framework Directive. Its purpose is to identify water bodies that can be categorised as heavily modified, particularly in response to significant dam construction throughout Spain over the past century (Fernández et al., 2012; Liu et al., 2022). Beyond its original use, some authors have used IAHRIS to assess the impact of climate change on water resources (Aznarez et al., 2021; Jiménez-Navarro et al., 2021; López-Ballesteros et al., 2020; Pérez-Sánchez et al., 2020). This study is the first to apply these indicators to evaluate the impact of land abandonment on river hydrological regimes. Furthermore, our aim is to assess and quantify the influence of climate variability and land–use changes on alterations to the hydrological regime.

2. Study Area

The Anduña River Basin (Figure 1) is located in the western area of the Pyrenees mountain range in Spain and covers an area of 4,728.61 ha. The terrain is orographically complex and is characterised by steep slopes, giving the study basin a wide elevation range from 801 m to 1,702 m. The climate is predominantly Atlantic, with two distinct peaks in precipitation occurring in autumn and spring (Amblar-Francés et al., 2020). On average, the area receives approximately 1,750 mm of annual precipitation. Due to its high altitude, the region experiences lower temperatures compared to its surroundings. The gauging station of Izalzu records a streamflow of 46.2 hm^3 per year annually, and the hydrological regime is characterised by minimum streamflow in the summer months and two maximum discharge peaks in January and March, which are driven by the precipitation regime, with a substantial constribution by snowmelt component in spring.

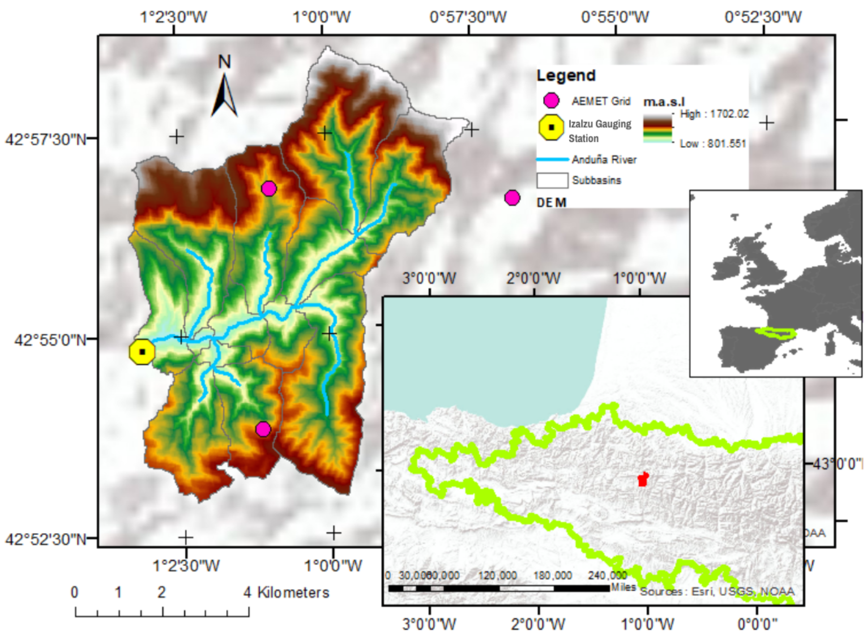

Figure 1: a) Location map of the Pyrenean region in Europe. b) Situation map of the Anduña River Basin in the Pyrenees. c) Digital elevation model (DEM) of the Anduña River basin and the location of Anduña gauging station.

Since 1956, land-use evolution in this region has been remarkable. In the 1950s, the region's population was primarily agrarian and rural, land-use mainly focused on agricultural and livestock activities with little mechanisation. Rain fed crops and large extensions of pastures and scrublands originating from extensive livestock farming predominated (Pardo et al., 2008). However, in subsequent decades, a massive abandonment of the countryside of the Pyrenees resulted in reforestation. Consequently, the land became predominantly occupied by forest (García-Ruiz et al., 1995), largely comprising conifers and hardwoods.

3. Methodology

Figure 2 presents a flowchart of the methodology employed in this study. The first step was to perform a Mann–Kendall trend analysis of the climatic variables for the historical period. Subsequently, a SWAT model was developed, calibrated and validated using observed daily flow data. The resulting SWAT model of the Anduña River basin was used to simulate Scenarios A, B and C. These scenarios simulated the effects of land–use change and climate variability on streamflow for the periods: 1956–1985 and 1986–2021. Scenario A was based on climate data for the period 1951-1985 and the 1956 land–use map, associated with the state before the region's transformation. Therefore, scenario A was the baseline scenario. Scenario B retained the land–use map before the massive reforestation process and incorporated climate data for the period 1986–2021, thus scenario B provided information on the change in hydrological variables caused by climate variability. Finally, scenario C, in addition to considering climate data for the period 1986–2021, updated the land–use map corresponding to the year 2000, thus this scenario accounted for changes produced by the combined effects of land–use change and climate variability.

The analysis examined changes in the hydrological cycle, focusing on runoff and PET, while utilising indicators of hydrological alteration (IHAs) to assess the extent of river modification(Fernández et al., 2012).

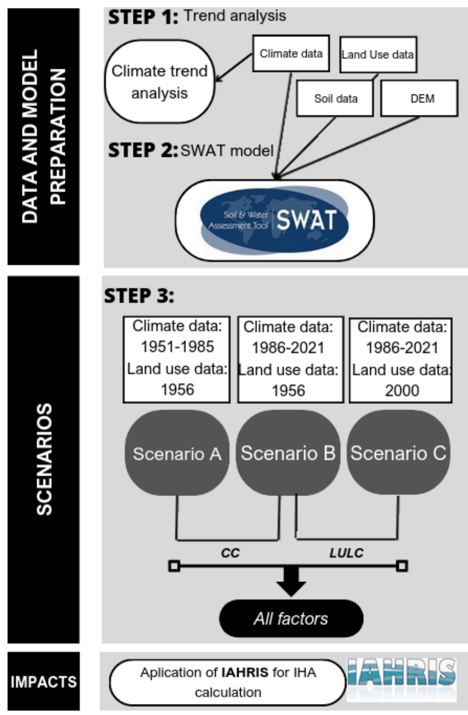

Figure 2: Flowchart of the methodology applied in this study

3.1. Trend analysis of climate variables

This study employed the Mann–Kendall test to identify trends in maximum and minimum temperatures, and precipitation during the historical period. The objective was to determine whether the time series exhibited consistent upward or downward trends, commonly referred to as monotonic trends. As a non-parametric test, it works with any distributions (i.e., the variable does not have to meet the assumption of normal distribution). The Mann–Kendall test has frequently been used to quantify the significance of trends in meteorological time series (Gocic and Trajkovic, 2013; Soltani and Mofidi, 2013). The Z-test is used to asses the presence or absence of significant trends; a negative (positive) Z-value refers to a negative (positive) trend. Moreover, Sens' slope (Sen, 1968) estimates the slope of linear trends providing information on the magnitude of the trends, and is less sensitive to outliers than other metrics. It is given for N pairs of data using the following expression:

$$Q_i = median(\frac{x_j - x_k}{j - k}) \;\; for\ i = 1, ..., N \quad (1)$$

where x_j and x_k are the data values at time j and k ($j \geq k$), respectively. Both methods have been applied using the Python package for the non-parametric Mann–Kendall family of trend tests.

3.2. SWAT model description

SWAT is a semi-distributed hydrological model that divided the basins of the study region into many sub-basins, further partitioned into hydrological response units (HRUs). Thus, the model considers the river network and its spatial heterogeneity (Arnold et al., 2012). Each HRU includes a combination of land cover, soil class, and slope. The SWAT model has been widely and successfully applied in watersheds with varying characteristics worldwide (Krysanova and White, 2015).

3.2.1. Input data for the hydrological modelling

The DEM data used as input for the SWAT model had a spatial resolution of 25 m x 25 m, obtained from the Spanish Geographical Institute (IGN, 2017). The soil dataset used in this study was the Harmonized World Soil

Map, with a spatial resolution of 1 km x 1 km (Nachtergaele et al., 2012). The climate and land-use data varied depending on the scenario. The climate data, comprising maximum temperature, minimum temperature, and precipitation data for 1951–1985 and 1986—2020, was obtained from the Spanish Meteorological Agency (AEMET) with a spatial resolution of 5 km x 5 km and a daily temporal frequency. Land-use maps from 1956 and 2000 were used as reference data for both historical periods. These were downloaded from the Government of Navarra regional sources. The six land-use types in the Anduña River Basin included bare soil, broad-leaved forest, coniferous forest evergreen, mixed forest, pasture, and shrub. Finally, discharge observations in the study catchment outlet (Izalzu, Figure 1) were acquired from the Government of Spain's Centre for Public Works Studies and Experimentation (CEDEX) website.

3.2.2. Calibration, validation, and evaluation of model performance

Sensitivity analysis and calibration of the SWAT model were developed using the SWAT-CUP program (Abbaspour et al., 2007) and its sequential uncertainty fitting algorithm SUFI-2. This tool allows SWAT users to perform automatic calibrations more efficiently and has been widely used by the SWAT community (Arnold et al., 2012). First, a global sensitivity analysis was conducted to identify the parameters with the most influence on streamflow. Of the parameters analysed in 500 iterations, those obtaining p-values lower than 0.005 were selected. Moreover, five snow-related parameters were considered in the calibration, due to the influence of snow dynamics on the hydrological cycle in the study area (Palazón and Navas, 2014). Automatic calibration was then applied to determine the values of the parameters that best reproduced the discharge considering the Kling–Gupta efficiency (KGE) as the objective function. In total, 1,000 simulations were run, initially 500 and then a further 500 using the adjusted parameter ranges.

The following five metrics were used to quantitatively evaluate the model's performance in the calibration and validation stages: the Nash–Sutcliffe efficiency (NSE), the root mean square Error (RMSE), the percent bias (PBIAS), the coefficient of determination (R^2), and the KGE, according to the recommended evaluation procedure established in Moriasi et al. (2015). The results of the model statistics were evaluated using the criteria proposed by (Kalin et al., 2010), which classify the results as very good, good, satisfactory, and unsatisfactory.

3.3. IAHRIS Software

One of the most common and complete methods of assessing riverine changes is calculating IHAs (Papadaki et al., 2016; López-Ballesteros et al., 2020). This method provides information on the degree of alteration between simulated and baseline scenarios. In this case, we evaluated the degree of alteration of the Anduña River Basin caused by climate variability and land-use change, allowing us to determine the contribution to the IHAs. This method was applied using IAHRIS version 2.2 software, which includes the 24 IHAs described in Table 1. Based on the most significant aspects of the flow regime (magnitude, frequency, variability, seasonality, and duration), IAHRIS establishes the IHA related to the maximum extreme (floods), minimum extreme (droughts), and usual values.

Table 1: List of IHAs using IAHRIS.

Components of the regime	Aspect	Indicator	Description
Usual values	Magnitude	M1	Magnitude of annual volume Magnitude of monthly volume
		M2	Magnitude of volume of the month: 12 values
		M3	Variability of annual volume
	Variability	V1	Variability of monthly volume
		V2	Variability of volume of the month: 12 values
		V3	Extreme variability
	Stationarity	E1	Seasonality of maximums
		E2	Seasonality of minimums
Maximum extreme values (floods)	Magnitude	IHA7	Magnitude of maximum floods
		IHA8	Magnitude of effective discharge
		IHA9	Magnitude of connectivity flow
		IHA10	Magnitude of usual floods
	Variability	IHA11	Variability of maximum floods
		IHA12	Variability of usual floods
	Duration	IHA13	Floods duration
	Seasonality	IHA14	Seasonality of floods (1 for each month)
Minimum extreme values (droughts)	Magnitude	IHA15	Magnitude of extreme droughts
		IHA16	Magnitude of usual droughts
	Variability	IHA17	Variability of extreme droughts
		IHA18	Variability of usual droughts
	Duration	IHA19	Duration of droughts
		IHA20	Number of days of null flow (1 for each month)
	Seasonality	IHA21	Seasonality of droughts (1 for each month)

IAHRIS uses 25 parameters to calculate the 24 IHA indicators, (Table 2) that quantitatively characterize the flow regime of a river: four for usual values, eight for floods, and seven for droughts. Within the scope of these

25 parameters, our study investigated those pertinent to flood characterisation. Our analysis focused on the following parameters: the average of the maximum daily flows throughout the year (Q_c), effective discharge (ED), conductivity discharge (CD), and flushing floods (FF). The ED is a geomorphic concept representing the flow, or range of flows that transport the most sediment over the long term, while the CD is a key indicator that enables the transport of aquatic life, organic matter, nutrients, and sediments to the floodplain and riparian system. Likewise, the FF is the flow corresponding to the mean curve of flows classified at the 5% exceedance percentile.

Additionally, each IHA represented a parameter change between the baseline and altered scenarios. In the case study, the alteration associated with the change from Scenario A to Scenario B was related to climate variability and from Scenario A to Scenario C to the combined effect of climate variability and land-use change. These alterations are hereafter referred to hereafter as 'Impact A-B' and 'Impact A-C', respectively. Indicators were calculated for each disturbance with values ranging from 0 to 1, where 1 indicated no disturbance and 0 indicated maximum disturbance (Swanson, 2002).

Table 2: List of parameters for calculating IHAs.

Components of the regime	Aspect	Parameter	Description	Resulting
Usual values	Magnitude and variability	H1	Mean (hm3)	M1
		H2	Median (hm3)	
		H3	Coefficient of variation	V1
		H4	Mean of the month (hm3): 12 values	M2
		H5	Median of the month (hm3): 12 values	M3
		H6	Coefficient of variation of the month: 12 values	V2
				V3
		H7	Extreme variability (hm3)	V4
	Seasonality	H8	Maximum relative frequency of the month: 12 values	E1
		H9	Minimum relative frequency of the month: 12 values	E2
	Variability	P4	Difference between the average flows associated with 10% and 90% percentiles	IHA3
Maximum extreme values (floods)	Magnitude and frequency	P5	Average of the maximum daily flows throughout the year	IHA7
		P6	Effective discharge	IHA8
		P7	Connectivity discharge	IHA9
		P8	Flushing flood (5% percentile)	IHA10
		P9	Coefficient of variation of the maximum daily flows throughout the year	IHA11
		P10	Coefficient of variation of the flushing flood series	IHA12
		P11	Consecutive days in a year with percentile below 5%	IHA13
		P12	Average number of days per month with percentile above 5%	IHA14
Minimum extreme values (droughts)	Magnitude and frequency	P13	Average of the minimum daily flows throughout the year	IHA15
		P14	Ordinary drought discharge (95% percentile)	IHA16
	Variability	P15	Coefficient of variation of the minimum daily flows throughout the year	IHA17
	Duration	P16	Coefficient of variation of the ordinary droughts series	IHA18
		P17	Consecutive days in a year with percentile below 95%	IHA19
		P18	Average number of days in the month with null flow	IHA20
	Seasonality	P19	Average number of days per month with percentile below 95%	IHA21

IAHRIS presented the results in three spider charts: one for usual values, one for floods, and one for droughts. IAHRIS obtained another indicator that provides information on global alteration (IGA) from the ratio between the areas of natural and altered scenarios depicted in the spider charts.

4. Results

4.1. Climate Variability

The results of the Mann–Kendall test and the Sen's slope are given in Table 3. Regarding the maximum and minimum temperatures during the historical period, we observed a positive trend throughout all the months of the year with a confidence level of 0.001 in the summer months (June, July, and August). The significance level is also maintained in the annual trend. However, no clear trend was observed for precipitation, consistent with those obtained in previous studies in the Pyrenees region, indicating to trends close to 0 and statistically non-significant in most cases (Juez et al., 2022; Lemus-Canovas et al., 2019). Lemus-Canovas et al. (2019), also obtained a slightly positive non-significant trend in the western region of the mountain range, where our study area is located.

Table 3: Trend analysis results. Test Z is the Mann–Kendall (MK) test statistic; Qi is the Sen's slope estimator. ** Indicates a significance level of 0.01, and *** indicates a significance level of 0.001

	Precipitation			Maximum Temperature			Minimum Temperature		
	Test Z	Sig.	Q_i	Test Z	Sig.	Q_i	Test Z	Sig.	Q_i
jan	1.350		0.028	2.134		0.019	2.809	**	0.028
feb	0.715		0.012	1.107		0.018	1.817		0.022
mar	0.745		0.012	1.191		0.016	1.995		0.015
apr	0.645		0.008	2.144		0.028	1.936		0.014
may	0.735		0.008	1.698		0.024	1.886		0.016
jun	-0.139		-0.002	3.743	***	0.046	4.070	***	0.027
jul	1.489		0.009	3.703	**	0.041	3.946	***	0.025
aug	0.010		0.000	3.345	***	0.041	4.358	***	0.028
sep	-0.199		-0.002	0.893		0.012	0.655		0.006
oct	0.705		0.012	2.144		0.026	3.018	**	0.025
nov	1.201		0.024	1.152		0.013	2.422		0.022
dec	0.000		0.000	1.102		0.012	1.648		0.015
annual	1.896	**	0.009	4.735	***	0.028	5.490	***	0.021

4.2. Land-use Change

LULC data for the past and baseline periods are given in Table 4. According to data for the year 1956, more than 43 % of the area was covered by pasture and more than 12 % was covered by scrubs, while the area occupied by the three forest types was 44 %. In contrast, the 2000 land-use map reveal a radically different picture, with forests extending over 73 % of the region and pastures and scrubs representing less than 30 %. This transformation is representative of socio–economic changes that occurred throughout the final decades of the 20th century in the region, which consisted of the abandonment of ploughed lands and subsequent plant succession which resulted in a reforested landscape (García-Ruiz et al., 1995; Poyatos et al., 2003; Lasanta et al., 2015, 2017).

Table 4: Surface area and percentage of cover of the six land-use types for the years 1956 and 2000.

Land Cover Type	Area Coverage km^2 (%)		Change (%)
	1956	2000	1956–2000
Bare Soil	15 (0.3%)	23 (0.5%)	0.23
Broad-leaved Forest	1604 (33.2%)	1872 (38.8%)	6.71
Coniferous Forest Evergreen	334 (6.9%)	1331 (27.5%)	19.62
Mixed Forest	171 (3.5%)	347 (7.2%)	5.61
Pasture	2101 (43.5%)	1075 (22.3%)	-22.60
Shrub	607 (12.6%)	183 (3.8%)	-9.88

4.3. Model Calibration and Validation

As discussed in the methodology section (Section 3), the sensitivity analysis did not consider snow-related parameters. The selected parameters are consistent with those identified in previous studies. Crucial similarities between sensitive parameters can be observed in Stratton et al. (2009), who explored sensitivity in a basin influenced by snow is explored, and Grusson et al. (2015), who studied a basin on the French side of the Pyrenees. Based on these and other studies of basins with similar characteristics (Palazón and Navas, 2014), the snow parameters given in Table 5 were incorporated into the calibration.

The NSE values for calibration and validation on a daily basis (Table 6) are considered satisfactory according to the criteria described by Kalin et al. (2010). Similarly, the PBIAS values, present very good results, since they remain below ±25 % and indicate only a slight tendency to overestimate the actual values. The remaining indices used to evaluate of the model's performance also gave satisfactory values: the R^2 is above 0.70 in both cases, while the KGE is above 0.55. These favourable results validate the SWAT

Table 5: Calibration parameters codes, descriptions, initial calibration range and final optimal values.

Parameter	Description	Calibration Range	Adjusted Value
Esco	Soil evaporation compensation factor	0 – 1	0,7543
Epco	Plant uptake compensation factor	0 – 1	0,7325
Cn_2	Initial SCS runoff curve number condition II	±20 %	-19.88
Awc	Available water capacity	±20 %	12.04
Snofall tmp	Snowfall temperature (ºC)	-5 – 5	0,491
Snomelt tmp	Snowmelt base temperature (∘C)	-5 – 5	2,465
Snomelt max	Maximum melt rate of snow during a year (mm ºC-1 day -1)	0 – 10	5,206
Snomelt min	Minimum melt rate of snow during a year (mm ºC-1 day -1)	0 – 10	1,276
Snomelt lag	Snow pack temperature lag factor	0 – 1	0,973

Table 6: Calibration and validation statistical values on a daily basis.

Period	R^2	NSE	PBIAS	KGE
Calibration (1992-2004)	0.72	0.51	-12.67	0.55
Validation (2005-2018)	0.75	0.55	-16.49	0.62

model of the Anduña River Basin for simulating daily flow in the scenarios described in the methodology section (Section 3).

Figure 3 gives the monthly time series of simulated and observed streamflow for the calibration and validation periods, observed monthly precipitation, and the values of the model performance evaluation statistics. The negative PBIAS indicate an overestimation of low flows (Figure 3). Despite this, Moriasi et al. (2015) propose that a PBIAS of less than 25% is acceptable for evaluating hydrological models. Recent reviews by Tan et al. (2021) support this criterion for SWAT model applications, while Mulligan (2013) suggests that physically based models, if accurately simulating current conditions, will likely perform well under scenario conditions. Moreover, Arabi et al. (2007) find that relative comparisons for land use scenarios yield consistent results with lower uncertainty. Therefore, despite inherent model uncertainties, we consider that the calibrated model is suitable for achieving our study objectives.

4.4. Impacts of landuse change and climate variability on the hydrological cycle

Table 7 presents the annual precipitation, mean annual runoff and evapotranspiration (ET) simulated by the SWAT model under scenarios A, B,

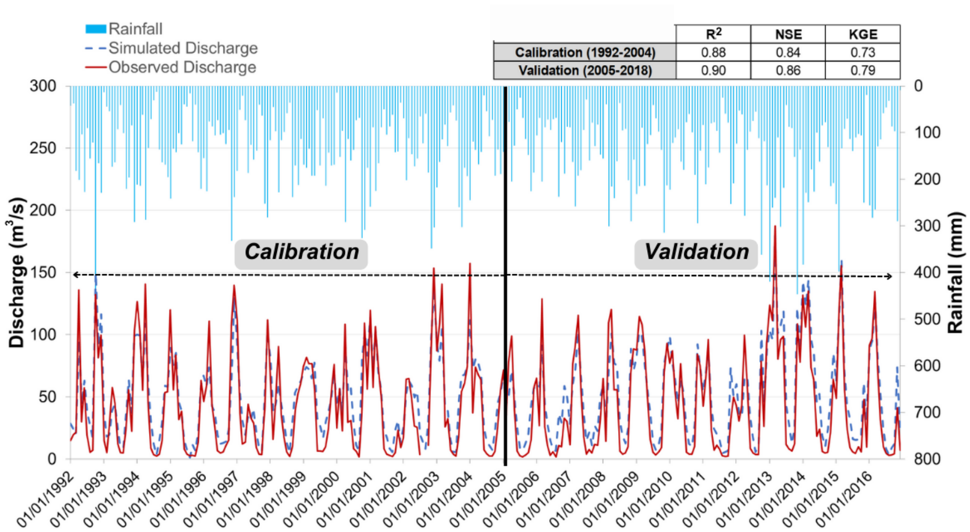

Figure 3: Monthly calibration and validation time-series and statistical values.

and C. From the comparison between scenarios A and B, we obtained information on the impact of climate variability on the hydrological cycle and observed that precipitation increases minimally, consistent with the trend analysis described in Section 4.1. Climate variability, also related to a rise in temperatures, increased ET by 15.5 mm and resulting in a decrease in runoff of 21.8 mm. The combined effect of climate variability and land-use change were obtained by comparing Scenarios A and C, which resulted in an increase in ET of 31 mm and a decrease in runoff of 36.12 mm. Therefore, the contribution of each factor in the increase of ET was 50 %. Concerning the decrease in runoff, the impacts of land-use change was almost as important as climate variability, contributing by 41.36 % while climate variability contributed by 58.64 %.

Table 7: Simulated average annual runoff, precipitation, PET, ET and percolation under scenarios A, B and C (mm).

Scenarios	P	PET	Percolation	ET	Runoff	Change ET	Change Runoff
A	1718.3	794.3	512.78	576.6	1100.2		
B	1722.2	836.7	481.71	592.1	1079.1	+15.5	-21.2
C	1722.2	836.7	467.23	607.6	1064.1	+31.0	-36.1

4.5. Impacts of land-use change and climate variability on the alterations hydrological regime

The results obtained using IAHRIS for the characterization of floods (Table 8) pointed to an increase in the magnitude of the maximum extreme events in the comparison of scenarios A and B. Overall, climate variability produced increases of more than 40 % in the variables Qc, ED and CD . The alteration of these variables is slightly mitigated by reforestation, leading to a decrease in values of 5 %, as observed in the results obtained for Scenario C, representing the combined effect of both factors on the hydrological regime.

Table 8: Flood parameters of IAHRIS over A, B and C scenarios. Q_c refers to the average of the maximum daily flows throughout the year, ED to effective discharge, CD to conductivity discharge, FF flushing floods and the CV expresses the variability of parameters

Scenarios	Q_c	ED	CD	FF	CV(Q_c)	CV(FF)
A	11.21	10.05	13.50	4.31	0.40	0.24
B	15.90	15.30	20.00	4.25	0.44	0.23
C	15.06	14.40	18.80	4.22	0.43	0.23

The changes in flood regimes translate into increases in the frequency and magnitude of flooding of the floodplain, directly influencing factors such as the availability of oxygen for plant roots, fundamental for the composition and productivity of riparian species and communities. Similarly, these changes can alter sediment erosion and deposition responsible for modulating the geomorphology of the floodplain surface, producing significant alterations in the successional dynamics of riparian ecosystems (Richter and Richter, 2000; LeRoy Poff and Allan, 1995).

4.6. Indicators of Hydrological Alteration

Figure 4 shows the results of IGA and spider-charts of IHA for the usual values, floods, and droughts, obtained using the IAHRIS method. The results are presented dissagregated into two different disturbances: impact A-B refers to the disturbance between scenarios A and B, while impact A-C describes the disturbance between scenarios A and C. Impact A-B reflects the contribution of climate variability in the alteration of the indicators, while impact A-C refers to the alteration caused by the combined effects of climate

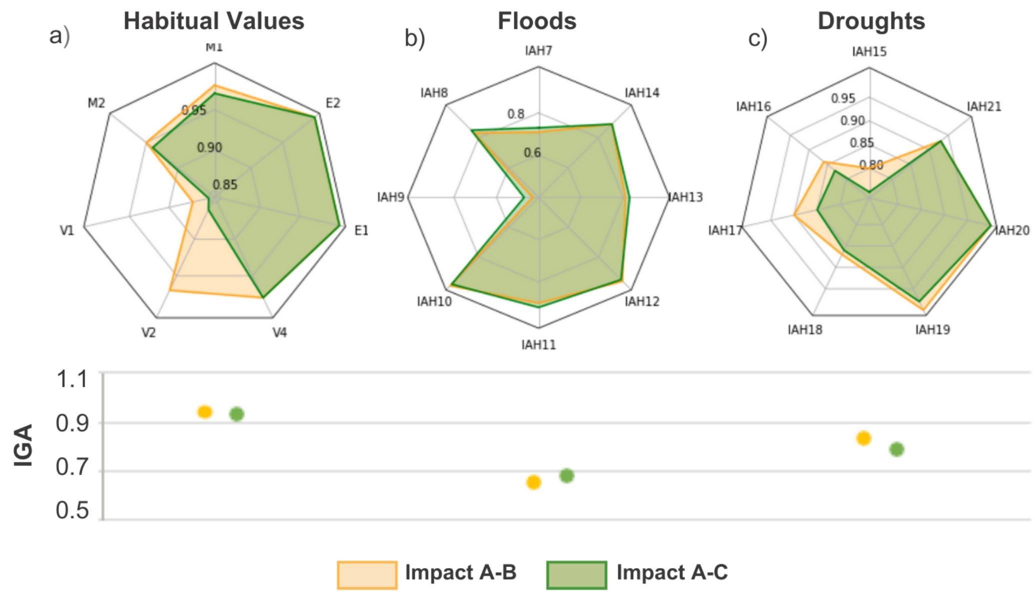

Figure 4: Spider charts of the IHAs and IGA values for habitual values, floods and droughts under impacts A–B and impact A–C.

variability and land-use changes.

Concerning the IGA indicators (Figure 4.b), a decrease in the quality of the water regime was observed, especially for floods: the IGA decreased to 0.65 due to climate variability, although this was slightly mitigated by the reforestation process, reaching 0.67. For the usual values and droughts, the IGA revealed higher values, above 0.8, indicating that the alteration was more subtle. Similarly, the results indicate that the combined effects of the climate and reforestation slightly increased the alteration in the usual values and droughts, contrasting with the results for floods.

The spider-charts (Figure 4.a) present the results of the indicators of hydrological alteration. Regarding the usual values, no indicator excessively influence the water regime, since all gave values higher than 0.80. We observed the greatest change in the variability of annual volume (V1) derived from climatic causes and accentuated by changes in land-use. However, the determining factor in the monthly volume variability (V2), was land-use change, causing the indicator's value to drop to 0.86. Changes in annual and interannual variability could influence the structure of ecosystem communities (Bêche et al., 2006). The indicators concerning to annual and monthly magnitude decreased slightly and the seasonality maxima and minima presented values close to 1, indicating minimal disturbance conditions. These conditions would be favourable for developing processes vital for habitat diversity and for stimulating germination and dispersal (Bêche et al., 2006).

The flood regime was the most altered of the analysed regimens, as the IGA indicates (Figure 4.b), the alteration was entirely due to climatic influences. This changes was slightly alleviated by reforestation. The most affected indicator was the frequency of connectivity flow (IHA9; Table 2), which is fundamental for enabling the transport of aquatic life, organic matter, nutrients, and sediments to the floodplain and riparian river system, as well as in maintaining adequate moisture conditions for species growth stages (Larsen et al., 2019). In addition, it is closely linked to successional dynamics, for example, by stimulating the rejuvenation of secondary channels and creating pond features that help maintain local plant and animal diversity in floodplains (Richter and Richter, 2000). The loss of connectivity with floodplains implies continuous ageing of the riparian habitat, endangering species renewal (Nilsson and Svedmark, 2002). The magnitude of maximum floods

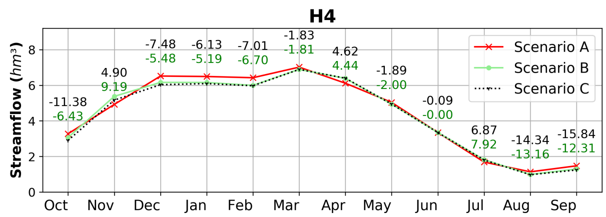

Figure 5: Monthly streamflow mean simulations under scenarios A, B and C with the changes expressed in percentages for scenario A–B (green) and for scenario A–C (black).

(IHA7) was the second most altered factor and the magnitude of effective discharge (IHA8) was also affected by climatic causes. Hence, the regeneration and flushing cycles of the usual flows would be affected along with the and sediment mobilisation transport processes responsible for riverbed geomorphology (Wohl et al., 2015).

Concerning droughts (Figure 4.c), the major alterations occurred in magnitude and frequency, which became more evident with the combined effects of climatic causes and reforestation. These predominantly affected the magnitude of extreme droughts (IHA15), the magnitude of usual droughts (IHA16), and the variability of extreme droughts (IHA17).

Figure 5 presents the mean monthly streamflow values under scenarios A, B, and C. The most significant decreases were observed in the winter, summer, and early autumn months. The decrease in winter was predominantly associated with climate variability accentuated by the influence of revegetation. The same trend occurred in summer and early autumn. This decrease would be associated with temperatures rise, illustrated in Table 3, which would cause an increase in ET. The greening process would accentuate this increase in ET by reducing streamflow.

The variability in streamflow for each month (H6) is displayed in Figure 6. We observed greater variability in the months with more precipitation for all scenarios. Increases were observed in March, June, and October due to the influence of climate variability, while a decrease in variability was observed during the winter months. Parameters H8 and H9 (Figure 6) provide information on the seasonality of maximum and minimum streamflow values,

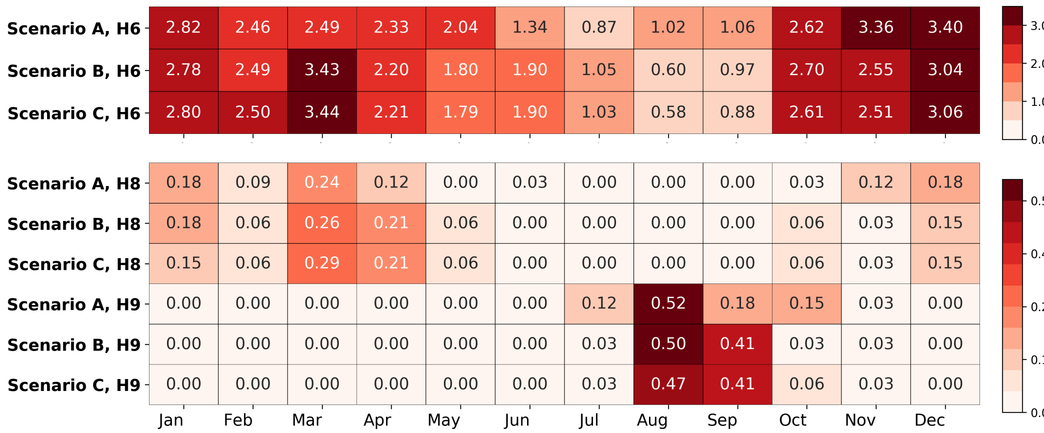

Figure 6: Monthly values for IAHRIS parameters under scenarios A, B and C

respectively, obtained for each month as the relative frequency or probability that the annual maximum and minimum monthly contribution occurs in that month (Martínez Santa-María and Fernández Yuste J.A., 2008). We observed that the probability of the annual maximum streamflow occurring in April increased almost two-fold due to the impact of climate variability. Similarly, climate variability altered the seasonality of the minimums. Therefore, the probability of the minimum occurring in September increased from 0.18 to 0.41. Climate variability caused a delay in the maximum and minimum for the hydrological regime in the Anduña River Basin. These alterations in the natural seasonal patterns of the water regime could produce distortions in the river functioning as an ecosystem due to the loss of synchrony with species' life cycles, affecting, among other things, reproductive patterns, migration, growth, and development, (Naiman et al., 2002) and favoring the progression of foreign species resulting in a biodiversity loss (Richter and Richter, 2000; Growns and Reinfelds, 2014).

5. Discussion

Examining the long-term time series data revealed a notable decline in runoff within the Anduña River Basin from 1951 to 2020. This trend aligns with similar observations documented for multiple catchments within the Pyrenees mountain region, as noted by Juez et al. (2022); Vicente-Serrano et al. (2021); López-Moreno et al. (2008). Additionally, analogous runoff reductions have been observed in other natural, non-managed catchments across the Iberian Peninsula, particularly those undergoing significant land–use transformations (Lorenzo-Lacruz et al., 2012; Vicente-Serrano et al., 2020).

Additionally, our analysis further quantifies the respective contributions of key factors underlying this decline in runoff, specifically climate variability and land-use change. Notably, our findings attribute nearly equal importance attributed to both factors, with contributions of 58.6% and 41.4%, respectively. These results substantiate the hypothesis posited by López-Moreno et al. (2008), supported by subsequent studies such as Juez et al. (2022), highlighting that the decline in streamflow magnitude cannot be solely ascribed to climate factors but is partially linked to greening processes in the Pyrenees. Our findings align with those of Vicente-Serrano et al. (2021). While the authors observed a more pronounced downward trend in streamflow that could be attributed to differing climatic conditions between the Mediterranean and Atlantic regions, they estimate that non-climate-related streamflow decline accounts for between 46% and 65% of the total reduction.

The peak flows analysis indicates an increase attributed to climate factors, in terms of magnitude and frequency, consistent with the findings of other studies conducted in mountainous basins (Roy et al., 2001; Stoffel et al., 2016). Braun et al. (2000) emphasized that flooding in mountain watersheds is frequently linked to intense precipitation and snowmelt during winter. However, this surge in stream flow is mitigated by the process of revegetation, which modulates the hydrological cycle's response to precipitation, not only in mean annual values but also in peak flows (Minang et al., 2015; Ranzi et al., 2002). Reforestation plays a crucial role in reducing flood risks by enhancing soil permeability through increased infiltration due to tree roots (Keeler et al., 2019) and heightened interception by forest canopies. These factors collectively contribute to minimising the hazards associated with flooding (Gallart and Llorens, 2004; Andréassian, 2004; Valente et al., 2021). Conversely, in cases of usual and extreme minimum streamflow (droughts), the reforestation process exacerbates alterations to the water regime, together with climatic causes.

Changes in these two determinants of water regime dynamics are expected to persist in the future. Specifically, rising temperatures and alterations in precipitation patterns are likely to significantly contribute to exacerbating changes in the water regime. Additionally, the process of land abandonment and the subsequent reforestation of agricultural lands could continue to spread. Coupled with the upward migration of forest boundaries due to increasing temperatures (López-Moreno et al., 2008; Beniston, 2003), this effect will likely enhance forest cover, intensifying impacts on the water regime. Given that climate variability is beyond the control of regional actors, developing land management plans aimed at reducing water consumption by vegetation is key to mitigating future impacts on the hydrological cycle. Llena et al. (2024) propose scrub cleaning as an effective measure with positive effects on surface runoff and hydrological connectivity in a Mediterranean basin in the Pyrenees. This practice would be useful for enhancing soil quality (Nadal-Romero et al., 2018) and help prevent forest fires (Lasanta et al., 2019). Furthermore, alternative silviculture practices such as thinning (Manrique-Alba et al., 2020), should be considered to adapt dense pine reforestation to new conditions in the context of climate change and protect hydrological regime.

6. Conclusions

This study used the SWAT model to quantify the contributions of climate variability and land–use change to alterations in the hydrological regime of a natural catchment in the Pyrenees region. The study conclusions are summarized as follows:(a) The SWAT model satisfactorily reproduced the hydrological dynamics of the Anduña River Basin obtaining the following statistics for the validation period: an R2 of 0.75, an NSE of 0.55, a PBIAS of -16.49 and KGE of 0.62. These results indicate a good performance of the model. (b) The climate trend analysis revealed a significant positive trend in the summer months for the maximum and minimum temperatures and in January and October for the minimum temperature. This significant trend is maintained on an annual scale. Regarding precipitation, no clear trend was identified on a monthly scale. However, a slight increase was precipitation is observed on an annual scale. (c) A radical transformation in the distribution of land–use in the basin, from a land dominated by pastures and shrubs to a basin were forests predominate, was observed. (d) Climate variability and greening process have decreased the mean annual streamflow in the Anduña

River Basin, with the contribution of climate variability being 58.6 %, while the contribution attributed to the greenness process is 41.1 %. (e) The results obtained by IAHRIS highlight an increase in the magnitude of maximum extreme events (floods) since an increase of 40 % in the variables Qc, ED, and CD due to climate variability was observed. Reforestation mitigated the alteration of these variables by approximately 5 %. (f) According to the IHAs, a degradation in the water regime was observed, especially in the case of floods. The degradation in the case of floods is caused by climate variability and alleviated as a consequence of the greening process. In the case of the usual values and droughts, the combination of climate and land-use change generated a greater alteration. (g) On a monthly scale, a modification in the magnitude, variability, and seasonality of the streamflow was observed, predominantly caused by climate variability.

7. Acknowledgements

We acknowledge support from the María de Maeztu Excellence Unit for the periods 2018-2022 (Ref. MDM-2017-0714) and 2023-2027 (Ref. CEX2021-001201-M funded by MCIN/AEI/10.13039/501100011033), including support from the KVORTEX predoctoral project (MDM-2017-0714-19-3). This research was also partly supported by the research project TwinTagus from the Spanish Ministry of Science and Innovation under grant PID2021-128126OA-I00. Javier Senent-Aparicio was also supported by the BC3 Visiting Programme – Talent Attraction.

References

Abbaspour, K., Vejdani, M., Haghighat, S., 2007. SWAT–CUP calibration and uncertainty programs for SWAT. International Congress on Modelling and Simulation 43, 1603–1609. doi:10.13031/2013.3000.

Amblar-Francés, M.P., Ramos-Calzado, P., Sanchis-Lladó, J., Hernanz-Lázaro, A., Peral-García, M.C., Navascués, B., Dominguez-Alonso, M., Pastor-Saavedra, M.A., Rodríguez-Camino, E., 2020. High resolution climate change projections for the Pyrenees region. Advances in Science and Research 17, 191–208. doi:10.5194/asr-17-191-2020.

Andréassian, V., 2004. Waters and forests: From historical controversy to scientific debate. Journal of Hydrology 291, 1–27. doi:10.1016/j.jhydrol.2003.12.015.

Arabi, M., Govindaraju, R.S., Hantush, M.M., 2007. A probabilistic approach for analysis of uncertainty in the evaluation of watershed management practices. Journal of Hydrology 333, 459–471. doi:10.1016/j.jhydrol.2006.09.012.

Arnell, N.W., 1999. The effect of climate change on hydrological regimes in Europe: A continental perspective. Global Environmental Change 9, 5–23. doi:10.1016/S0959-3780(98)00015-6.

Arnold, J.G., Moriasi, D.N., Gassman, P.W., Abbaspour, K.C., White, M.J., Srinivasan, R., Santhi, C., Harmel, R.D., Van Griensven, A., Van Liew, M.W., Kannan, N., Jha, M.K., 2012. SWAT: Model use, calibration, and validation. Transactions of the ASABE 55, 1491–1508.

Aznarez, C., Jimeno-Sáez, P., López-Ballesteros, A., Pacheco, J.P., Senent-Aparicio, J., 2021. Analysing the impact of climate change on hydrological ecosystem services in laguna del sauce (Uruguay) using the swat model and remote sensing data. Remote Sensing 13. doi:10.3390/rs13102014.

Bêche, L.A., McElravy, E.P., Resh, V.H., 2006. Long-term seasonal variation in the biological traits of benthic-macroinvertebrates in two Mediterranean-climate streams in California, U.S.A. Freshwater Biology 51, 56–75. doi:10.1111/j.1365-2427.2005.01473.x.

Beguería, S., López-Moreno, J.I., Lorente, A., Seeger, M., García-Ruiz, J.M., 2003. Assessing the effect of climate oscillations and land-use changes on streamflow in the Central Spanish Pyrenees. Ambio 32, 283–286. doi:10.1579/0044-7447-32.4.283.

Beniston, M., 2003. Climatic Change in Mountain Regions: A Review of Possible Impacts. Climatic Change , 5–31doi:10.1007/978-94-015-1252-7.

Boix-Fayos, C., Boerboom, L.G., Janssen, R., Martínez-Mena, M., Almagro, M., Pérez-Cutillas, P., Eekhout, J.P., Castillo, V., de Vente, J., 2020. Mountain ecosystem services affected by land use changes and hydrological control works in Mediterranean catchments. Ecosystem Services 44, 101136. URL: `https://doi.org/10.1016/j.ecoser.2020.101136`, doi:10.1016/j.ecoser.2020.101136.

Braun, L.N., Weber, M., Schulz, M., 2000. Consequences of climate change for runoof from Alpine regions. Annals of Glaciology 31, 19–25. doi:10.3189/172756400781820165.

FAO, 2014. State of the world's forests 2014: Enhancing the socioeconomic benefits from forests.

Fernández, J.A., Martínez, C., Magdaleno, F., 2012. Application of indicators of hydrologic alterations in the designation of heavily modified water bodies in Spain. Environmental Science and Policy 16, 31–43. doi:10.1016/j.envsci.2011.10.004.

Gallart, F., Llorens, P., 2004. Observations on land cover changes and water resources in the headwaters of the Ebro catchment, Iberian Peninsula. Physics and Chemistry of the Earth 29, 769–773. doi:10.1016/j.pce.2004.05.004.

García-Ruiz, J.M., Lasanta, T., Ortigosa, L., Ruiz-Flaño, P., Martí-Bono, C., González, C., 1995. Sediment Yield under Different Land Uses in the Spanish Pyrenees . International Mountain Society 15, 229–240.

Gocic, M., Trajkovic, S., 2013. Analysis of changes in meteorological variables using Mann-Kendall and Sen's slope estimator statistical tests in Serbia. Global and Planetary Change 100, 172–182. URL: `http://dx.doi.org/10.1016/j.gloplacha.2012.10.014`, doi:10.1016/j.gloplacha.2012.10.014.

Growns, I., Reinfelds, I., 2014. Environmental flow management using transparency and translucency rules. Marine and Freshwater Research 65, 667–673. doi:10.1071/MF13192.

Grusson, Y., Sun, X., Gascoin, S., Sauvage, S., Raghavan, S., Anctil, F., Sáchez-Pérez, J.M., 2015. Assessing the capability of the SWAT model to simulate snow, snow melt and streamflow dynamics over an alpine watershed. Journal of Hydrology 531, 574–588. URL: `http://dx.doi.org/10.1016/j.jhydrol.2015.10.070`, doi:10.1016/j.jhydrol.2015.10.070.

Guo, S., Tian, L., Chen, S., Liang, J., Tian, J., Cao, B., Wang, X., He, C., 2024. Analysis of effects of vegetation cover and elevation on water yield in an alpine basin of the Qilian Mountains in Northwest China by integrating the WRF-Hydro and Budyko framework. Journal of Hydrology 629, 130580. URL: https://doi.org/10.1016/j.jhydrol.2023.130580, doi:10.1016/j.jhydrol.2023.130580.

Haria, A.H., Price, D.J., 2000. Evaporation from Scots pine (Pinus sylvestris) following natural re-colonisation of the Cairngorm mountains, Scotland. Hydrology and Earth System Sciences 4, 451–461. URL: https://hess.copernicus.org/articles/4/451/2000/, doi:10.5194/hess-4-451-2000.

IGN, 2017. Plan nacional de ortofotografía aérea. http://pnoa.ign.es/, (accessed on 3 January 2023). (In Spanish) (In Spanish).

Immerzeel, W.W., Lutz, A.F., Andrade, M., Bahl, A., Biemans, H., Bolch, T., Hyde, S., Brumby, S., Davies, B.J., Elmore, A.C., Emmer, A., Feng, M., Fernández, A., Haritashya, U., Kargel, J.S., Koppes, M., Kraaijenbrink, P.D., Kulkarni, A.V., Mayewski, P.A., Nepal, S., Pacheco, P., Painter, T.H., Pellicciotti, F., Rajaram, H., Rupper, S., Sinisalo, A., Shrestha, A.B., Viviroli, D., Wada, Y., Xiao, C., Yao, T., Baillie, J.E., 2020. Importance and vulnerability of the world's water towers. Nature 577, 364–369. URL: http://dx.doi.org/10.1038/s41586-019-1822-y, doi:10.1038/s41586-019-1822-y.

Jiménez-Navarro, I.C., Jimeno-Sáez, P., López-Ballesteros, A., Pérez-Sánchez, J., Senent-Aparicio, J., 2021. Impact of climate change on the hydrology of the forested watershed that drains to lake erken in sweden: An analysis using swat+ and cmip6 scenarios. Forests 12. doi:10.3390/f12121803.

Juez, C., Garijo, N., Nadal-Romero, E., Vicente-Serrano, S.M., 2022. Wavelet analysis of hydro-climatic time-series and vegetation trends of the Upper Aragón catchment (Central Spanish Pyrenees). Journal of Hydrology 614, 128584. URL: https://doi.org/10.1016/j.jhydrol.2022.128584, doi:10.1016/j.jhydrol.2022.128584.

Kalin, L., Isik, S., Schoonover, J.E., Lockaby, B.G., 2010. Predicting Water Quality in Unmonitored Watersheds Using Artificial Neural Networks. Journal of Environmental Quality 39, 1429–1440. doi:10.2134/jeq2009.0441.

Keeler, B.L., Hamel, P., McPhearson, T., Hamann, M.H., Donahue, M.L., Meza Prado, K.A., Arkema, K.K., Bratman, G.N., Brauman, K.A., Finlay, J.C., Guerry, A.D., Hobbie, S.E., Johnson, J.A., MacDonald, G.K., McDonald, R.I., Neverisky, N., Wood, S.A., 2019. Social-ecological and technological factors moderate the value of urban nature. Nature Sustainability 2, 29–38. URL: `http://dx.doi.org/10.1038/s41893-018-0202-1`, doi:10.1038/s41893-018-0202-1.

Krysanova, V., White, M., 2015. Aperçu des progrès de l'évaluation des ressources en eau avec SWAT. Hydrological Sciences Journal 60, 771–783. URL: `http://dx.doi.org/10.1080/02626667.2015.1029482`, doi:10.1080/02626667.2015.1029482.

Larsen, S., Karaus, U., Claret, C., Sporka, F., Hamerlík, L., Tockner, K., 2019. Flooding and hydrologic connectivity modulate community assembly in a dynamic river-floodplain ecosystem. PLoS ONE 14, 1–22. doi:10.1371/journal.pone.0213227.

Lasanta, T., Arnáez, J., Pascual, N., Ruiz-Flaño, P., Errea, M.P., Lana-Renault, N., 2017. Space–time process and drivers of land abandonment in Europe. Catena 149, 810–823. URL: `http://dx.doi.org/10.1016/j.catena.2016.02.024`, doi:10.1016/j.catena.2016.02.024.

Lasanta, T., Nadal-Romero, E., Arnáez, J., 2015. Managing abandoned farmland to control the impact of re-vegetation on the environment. The state of the art in Europe. Environmental Science and Policy 52, 99–109. doi:10.1016/j.envsci.2015.05.012.

Lasanta, T., Nadal-Romero, E., García-Ruiz, J.M., 2019. Clearing shrubland as a strategy to encourage extensive livestock farming in the Mediterranean Mountains. Geographical Research Letters 45, 487–513. doi:10.18172/cig.3616.

Lemus-Canovas, M., Lopez-Bustins, J.A., Trapero, L., Martin-Vide, J., 2019. Combining circulation weather types and daily precipitation modelling to derive climatic precipitation regions in the Pyrenees. Atmospheric Research 220, 181–193. URL: `https://doi.org/10.1016/j.atmosres.2019.01.018`, doi:10.1016/j.atmosres.2019.01.018.

LeRoy Poff, N., Allan, J.D., 1995. Functional organization of stream fish assemblages in relation to hydrological variability. Ecology 76, 606–627. doi:10.2307/1941217.

Liu, S., Pérez-Sánchez, J., Jimeno-Sáez, P., Alcalá, F.J., Senent-Aparicio, J., 2022. A novel approach to assessing the impacts of dam construction on hydrologic and ecosystem alterations. Case study: Castril river basin, Spain. Ecohydrology and Hydrobiology 22, 598–608. URL: https://doi.org/10.1016/j.ecohyd.2022.08.004, doi:10.1016/j.ecohyd.2022.08.004.

Llena, M., Nadal-Romero, E., Zabalza-Martínez, J., Cortijos-López, M., Lasanta, T., 2024. Effects of post-abandonment management on surface runoff in a Mediterranean mid-mountain basin. Catena 237. doi:10.1016/j.catena.2023.107775.

López-Ballesteros, A., Senent-Aparicio, J., Martínez, C., Pérez-Sánchez, J., 2020. Assessment of future hydrologic alteration due to climate change in the Aracthos River basin (NW Greece). Science of the Total Environment 733, 139299. URL: https://doi.org/10.1016/j.scitotenv.2020.139299, doi:10.1016/j.scitotenv.2020.139299.

López-Moreno, J.I., Beniston, M., García-Ruiz, J.M., 2008. Environmental change and water management in the Pyrenees: Facts and future perspectives for Mediterranean mountains. Global and Planetary Change 61, 300–312. doi:10.1016/j.gloplacha.2007.10.004.

López-Moreno, J.I., García-Ruiz, J.M., 2004. Influence of snow accumulation and snowmelt on streamflow in the central Spanish Pyrenees / Influence de l'accumulation et de la fonte de la neige sur les écoulements dans les Pyrénées centrales espagnoles. Hydrological Sciences Journal 49. doi:10.1623/hysj.49.5.787.55135.

López-Moreno, J.I., Vicente-Serrano, S.M., Moran-Tejeda, E., Zabalza, J., Lorenzo-Lacruz, J., García-Ruiz, J.M., 2011. Impact of climate evolution and land use changes on water yield in the ebro basin. Hydrology and Earth System Sciences 15, 311–322. doi:10.5194/hess-15-311-2011.

Lorenzo-Lacruz, J., Vicente-Serrano, S.M., López-Moreno, J.I., Morán-Tejeda, E., Zabalza, J., 2012. Recent trends in Iberian streamflows (1945-2005). Journal of Hydrology 414-415, 463–475. URL: http://dx.doi.org/10.1016/j.jhydrol.2011.11.023, doi:10.1016/j.jhydrol.2011.11.023.

Manrique-Alba, À., Beguería, S., Molina, A.J., González-Sanchis, M., Tomàs-Burguera, M., del Campo, A.D., Colangelo, M., Camarero, J.J., 2020. Long-term thinning effects on tree growth, drought response and water use efficiency at two Aleppo pine plantations in Spain. Science of the Total Environment 728, 138536. URL: https://doi.org/10.1016/j.scitotenv.2020.138536, doi:10.1016/j.scitotenv.2020.138536.

Martinez, C., Fernández, J., 2010. Iahris 2.2 indicators of hydrologic alteration in rivers: Free software. Ministerio de Medio Ambiente. Universidad Politécnica de Madrid .

Martínez-Fernández, J., Sánchez, N., Herrero-Jiménez, C.M., 2013. Recent trends in rivers with near-natural flow regime: The case of the river headwaters in Spain. Progress in Physical Geography 37, 685–700. doi:10.1177/0309133313496834.

Martínez Santa-María, C., Fernández Yuste J.A., 2008. Índices de Alteración Hidrológica en Ríos (IAHRIS). Manual de Referencia Metodológica Versión 1. Ministerio de Medio Ambiente. Universidad Politécnica de Madrid , 1–69URL: http://www.chduero.es/acciona5/metodologia/iharis.pdf.

Mellado-Díaz, A., Sánchez-González, J.R., Guareschi, S., Magdaleno, F., Toro Velasco, M., 2019. Exploring longitudinal trends and recovery gradients in macroinvertebrate communities and biomonitoring tools along regulated rivers. Science of the Total Environment 695, 133774. URL: https://doi.org/10.1016/j.scitotenv.2019.133774, doi:10.1016/j.scitotenv.2019.133774.

Minang, P.A., van Noordwijk, M., Freeman, O.E., Mbow, C., de Leeuw, J., Catacutan, 2015. Climate-Smart Landscapes: Multifunctionality In Practice. Nairobi, Kenya:World Agroforestry Centre (ICRAF). World Agroforestry Centre , 404.

Molina-Navarro, E., Trolle, D., Martínez-Pérez, S., Sastre-Merlín, A., Jeppesen, E., 2014. Hydrological and water quality impact assessment of a Mediterranean limno-reservoir under climate change and land use management scenarios. Journal of Hydrology 509, 354–366. URL: `http://dx.doi.org/10.1016/j.jhydrol.2013.11.053`, doi:10.1016/j.jhydrol.2013.11.053.

Moriasi, D.N., Gitau, M.W., Pai, N., Daggupati, P., 2015. Hydrologic and water quality models: Performance measures and evaluation criteria. Transactions of the ASABE 58, 1763–1785. doi:10.13031/trans.58.10715.

Nachtergaele, F., Van Velthuizen, H., Verelst, L., Wiberg, D., 2012. Harmonized world soil database. IIASA version 1.2. doi:–.

Nadal-Romero, E., Juez, C., Khorchani, M., Peña-Angulo, D., Lana-Renault, N., Regüés, D., Lasanta, T., García-Ruiz, J.M., 2021. Impacts of Land Abandonment on Flood Mitigation in Mediterranean Mountain Areas. doi:10.1007/698-2021-772.

Nadal-Romero, E., Peña-Angulo, D., Regues, D., 2018. Rainfall, run-off, and sediment transport dynamics in a humid mountain badland area: Long-term results from a small catchment. Hydrological Processes 32, 1588–1606. doi:10.1002/hyp.11495.

Naiman, R.J., Bunn, S.E., Nilsson, C., Petts, G.E., Pinay, G., Thompson, L.C., 2002. Legitimizing fluvial ecosystems as users of water: An overview. Environmental Management 30, 455–467. doi:10.1007/s00267-002-2734-3.

Nilsson, C., Svedmark, M., 2002. Basic principles and ecological consequences of changing water regimes: Riparian plant communities. Environmental Management 30, 468–480. doi:10.1007/s00267-002-2735-2.

Palazón, L., Navas, A., 2014. Modeling sediment sources and yields in a Pyrenean catchment draining to a large reservoir (Ésera River, Ebro Basin). Journal of Soils and Sediments 14, 1612–1625. doi:10.1007/s11368-014-0911-7.

Papadaki, C., Soulis, K., Muñoz-Mas, R., Martinez-Capel, F., Zogaris, S., Ntoanidis, L., Dimitriou, E., 2016. Potential impacts of climate change on flow regime and fish habitat in mountain rivers of the south-western Balkans. Science of the Total Environment 540, 418–428. URL: http://dx.doi.org/10.1016/j.scitotenv.2015.06.134, doi:10.1016/j.scitotenv.2015.06.134.

Pardo, F., Velasco, A., Gil, L., 2008. Tercer Inventario Forestal Nacional 1997-2007: La Tranformación Histórica del Paisaje Forestal en Navarra. Ministerio de Medio Ambiente, Gobierno de España 2, 7–19. doi:–.

Pérez-Sánchez, J., Senent-Aparicio, J., Santa-María, C.M., López-Ballesteros, A., 2020. Assessment of ecological and hydro-geomorphological alterations under climate change using SWAT and IAHRIS in the Eo River in Northern Spain. Water (Switzerland) 12. doi:10.3390/W12061745.

Poyatos, R., Latron, J., Llorens, P., 2003. Land use and land cover change after agricultural abandonment: The case of a Mediterranean Mountain area (Catalan Pre-Pyrenees). Mountain Research and Development 23, 362–368. doi:10.1659/0276-4741(2003)023[0362:LUALCC]2.0.CO;2.

Ranzi, R., Bochicchio, M., Bacchi, B., 2002. Effects on floods of recent afforestation and urbanisation in the Mella River (Italian Alps). Hydrology and Earth System Sciences 6, 239–254. URL: https://hess.copernicus.org/articles/6/239/2002/, doi:10.5194/hess-6-239-2002.

Ranzi, R., Caronna, P., Tomirotti, M., 2017. Impact of Climatic and Land Use Changes on River Flows in the Southern Alps. Springer Singapore, Singapore. pp. 61–83. URL: https://doi.org/10.1007/978-981-10-2051-3-3, doi:10.1007/978-981-10-2051-3-3.

Rasouli, K., Pomeroy, J., Whitfield, P., 2019a. Hydrological responses of headwater basins to monthly perturbed climate in the north american cordillera. Journal of Hydrometeorology 20. doi:10.1175/JHM-D-18-0166.1.

Rasouli, K., Pomeroy, J.W., Whitfield, P.H., 2019b. Are the effects of vegetation and soil changes as important as climate change impacts on hydrological processes? Hydrology and Earth System Sciences 23, 4933–4954. doi:10.5194/hess-23-4933-2019.

Richter, B.D., Richter, H.E., 2000. Society for Conservation Biology Prescribing Flood Regimes to Sustain Riparian Ecosystems along Meandering Rivers Published by : Wiley for Society for Conservation Biology Linked references are available on JSTOR for this article : Prescribing Flood Regim. Wiley for Society for Conservation Biology 14, 1467–1478.

Roy, L., Leconte, R., Brissette, F.P., Marche, C., 2001. The impact of climate change on seasonal floods of a Southern Quebec river basin. Hydrological Processes 15, 3167–3179. doi:10.1002/hyp.323.

Sanmiguel-Vallelado, A., Morán-Tejeda, E., Alonso-González, E., López-Moreno, J.I., 2017. Effect of snow on mountain river regimes: an example from the Pyrenees. Frontiers of Earth Science 11, 515–530. doi:10.1007/s11707-016-0630-z.

Sen, P.K., 1968. Estimates of the Regression Coefficient Based on Kendall's Tau. Journal of the American Statistical Association 63, 1379–1389. doi:10.1080/01621459.1968.10480934.

Senent-Aparicio, J., Liu, S., Pérez-Sánchez, J., López-Ballesteros, A., Jimeno-Sáez, P., 2018. Assessing impacts of climate variability and reforestation activities on water resources in the headwaters of the Segura River Basin (SE Spain). Sustainability (Switzerland) 10. doi:10.3390/su10093277.

Soltani, M., Mofidi, A., 2013. Using Mann-Kendall and time series techniques forstatistical analysisof long-term precipitation in gorgan weather station. World Applied Sciences Journal 28, 902–908. doi:10.5829/idosi.wasj.2013.28.07.946.

Stewart, I.T., Cayan, D.R., Dettinger, M.D., 2005. Changes toward earlier streamflow timing across western North America. Journal of Climate 18, 1136–1155. doi:10.1175/JCLI3321.1.

Stoffel, M., Wyżga, B., Marston, R.A., 2016. Floods in mountain environments: A synthesis. Geomorphology 272, 1–9. doi:10.1016/j.geomorph.2016.07.008.

Stratton, B.T., Sridhar, V., Gribb, M.M., McNamara, J.P., Narasimhan, B., 2009. Modeling the spatially varying water balance processes in a Semiarid Mountainous Watershed of Idaho. Journal of the American Water Resources Association 45, 1390–1408. doi:10.1111/j.1752-1688.2009.00371.x.

Swanson, S., 2002. Indicators of hydrologic alteration. Bureau of Land Management Resource Notes 0, 2.

Tan, M.L., Gassman, P.W., Liang, J., Haywood, J.M., 2021. A review of alternative climate products for SWAT modelling: Sources, assessment and future directions. Science of the Total Environment 795, 148915. URL: https://doi.org/10.1016/j.scitotenv.2021.148915, doi:10.1016/j.scitotenv.2021.148915.

Tasser, E., Walde, J., Tappeiner, U., Teutsch, A., Noggler, W., 2007. Land-use changes and natural reforestation in the Eastern Central Alps. Agriculture, Ecosystems and Environment 118, 115–129. URL: https://www.sciencedirect.com/science/article/pii/S0167880906001575, doi:https://doi.org/10.1016/j.agee.2006.05.004.

Valente, M.L., Reichert, J.M., Cavalcante, R.B.L., Minella, J.P.G., Evrard, O., Srinivasan, R., 2021. Afforestation of degraded grasslands reduces sediment transport and may contribute to streamflow regulation in small catchments in the short-run. Catena 204. doi:10.1016/j.catena.2021.105371.

Vicente-Serrano, S.M., Domínguez-Castro, F., Murphy, C., Peña-Angulo, D., Tomas-Burguera, M., Noguera, I., López-Moreno, J.I., Juez, C., Grainger, S., Eklundh, L., Conradt, T., Azorin-Molina, C., El Kenawy, A., 2021. Increased Vegetation in Mountainous Headwaters Amplifies Water Stress During Dry Periods. Geophysical Research Letters 48, 1–10. doi:10.1029/2021GL094672.

Vicente-Serrano, S.M., McVicar, T.R., Miralles, D.G., Yang, Y., Tomas-Burguera, M., 2020. Unraveling the influence of atmospheric evaporative demand on drought and its response to climate change. Wiley Interdisciplinary Reviews: Climate Change 11, 1–31. doi:10.1002/wcc.632.

Viviroli, D., Dürr, H.H., Messerli, B., Meybeck, M., Weingartner, R., 2007. Mountains of the world, water towers for humanity: Typology, mapping, and global significance. Water Resources Research 43, 1–13. doi:10.1029/2006WR005653.

Wohl, E., Bledsoe, B.P., Jacobson, R.B., Poff, N.L., Rathburn, S.L., Walters, D.M., Wilcox, A.C., 2015. The natural sediment regime in rivers: Broadening the foundation for ecosystem management. BioScience 65, 358–371. doi:10.1093/biosci/biv002.

Yin, Z., Feng, Q., Yang, L., Wen, X., Si, J., Zou, S., 2017. Long term quantification of climate and land cover change impacts on streamflow in an alpine river catchment, northwestern China. Sustainability (Switzerland) 9. doi:10.3390/su9071278.

Zeng, Z., Zhu, Z., Lian, X., Li, L.Z., Chen, A., He, X., Piao, S., 2016. Responses of land evapotranspiration to Earth's greening in CMIP5 Earth System Models. Environmental Research Letters 11. doi:10.1088/1748-9326/11/10/104006.

Zhang, L., Karthikeyan, R., Bai, Z., Srinivasan, R., 2017. Analysis of streamflow responses to climate variability and land use change in the Loess Plateau region of China. Catena 154, 1–11. URL: http://dx.doi.org/10.1016/j.catena.2017.02.012, doi:10.1016/j.catena.2017.02.012.